PICTURE OF THE MONTH

Some Frequently Overlooked Severe Thunderstorm Characteristics Observed on GOES Imagery: A Topic for Future Research

JOHN F. WEAVER AND DAN LINDSEY

NOAA/NESDIS/RAMM Team, Cooperative Institute for Research in the Atmosphere, Colorado State University, Fort Collins, Colorado

23 October 2003 and 23 December 2003

ABSTRACT

Several examples of Geostationary Operational Environmental Satellite (GOES) visible satellite images depicting cloud features often associated with the transition to, or intensification of, supercell thunderstorms are presented. The accompanying discussion describes what is known about these features, and what is left to learn. The examples are presented to increase awareness among meteorologists of these potentially significant storm features.

1. Introduction

The role of satellite imagery in defining the near-storm environment of severe/tornadic thunderstorms has been well documented over the past three decades (Purdom 1976, 1983; Weaver 1980; Weaver and Nelson 1982; Purdom and Scofield 1986; Weaver and Purdom 1995; Browning et al. 1997; Weaver et al. 1994, 2000; 2002; Bikos et al. 2002). Additionally, several papers have been written concerning storm-top characteristics of severe storms (Heymsfield et al. 1983; McCann 1983; Adler and Mack 1986; Setvák and Doswell 1991). Much less has been written concerning low-level, severe-thunderstorm structure as observed on visible satellite im-

Corresponding author address: John F. Weaver, NOAA/NESDIS/RAMM, CIRA Building—Foothills Campus, Colorado State University, Fort Collins, CO 80523.
E-mail: weaver@cira.colostate.edu

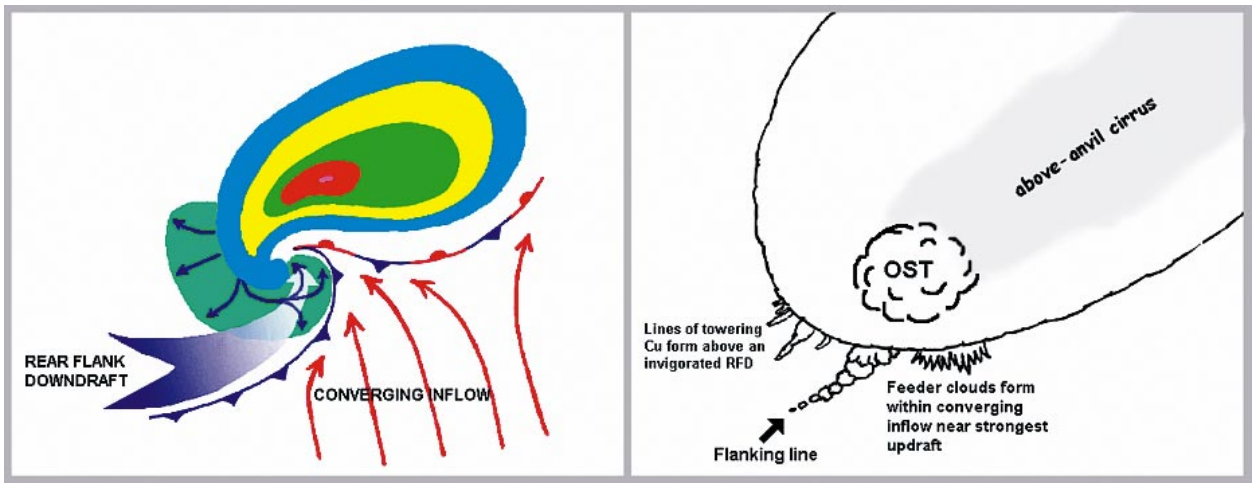

FIG. 1. Schematic diagram of certain aspects of a supercell thunderstorm: (left) idealized, base-reflectivity radar echo, the location of the descending rear-flank downdraft (RFD), the associated cold air at the surface (green), converging low-level inflow streamlines, and quasi-stationary, storm-related fronts, and (right) visible satellite representation of the same storm showing the overshooting top (OST), above-anvil cirrus, cumulus congestus above the rear-flank outflow (i.e., the flanking line), lines of towering cumulus over the new or invigorated RFD, and short compact lines of cumulus congestus towers associated with the intense inflow.

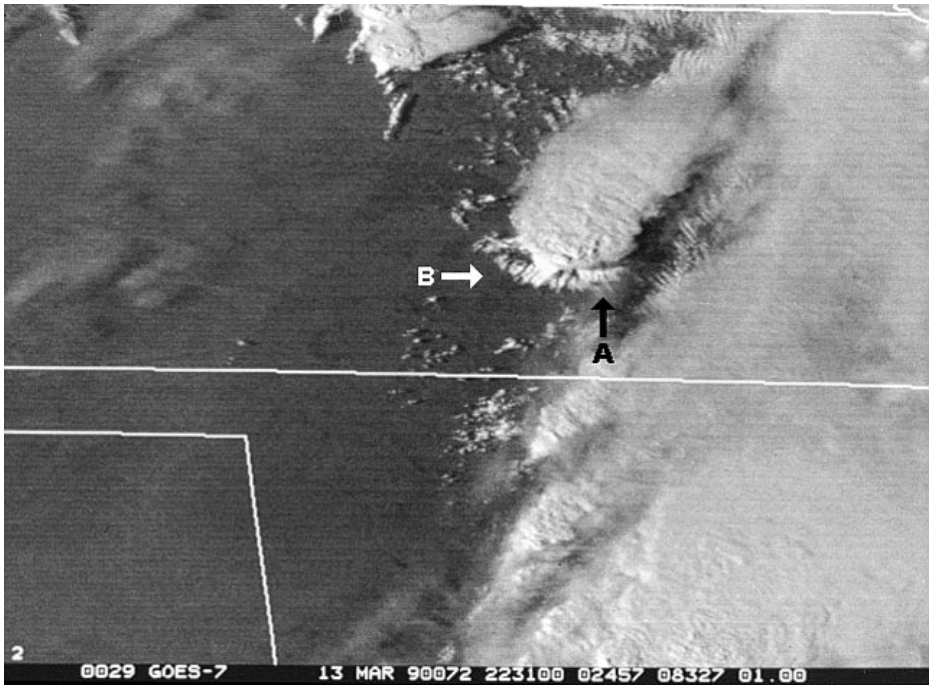

FIG. 2. *Geostationary Operational Environmental Satellite-7* (*GOES-7*) visible satellite image from 13 Mar 1990 at 2231 UTC over southern Kansas. Image shows a supercell thunderstorm just before it produces an F5 tornado in Hesston, KS. Arrow A points to compact lines of towering cumulus—or feeder clouds—associated with the storm's intense inflow; arrow B points to lines of towering cumulus forming above a newly formed rear-flank downdraft upstream from the primary flanking line.

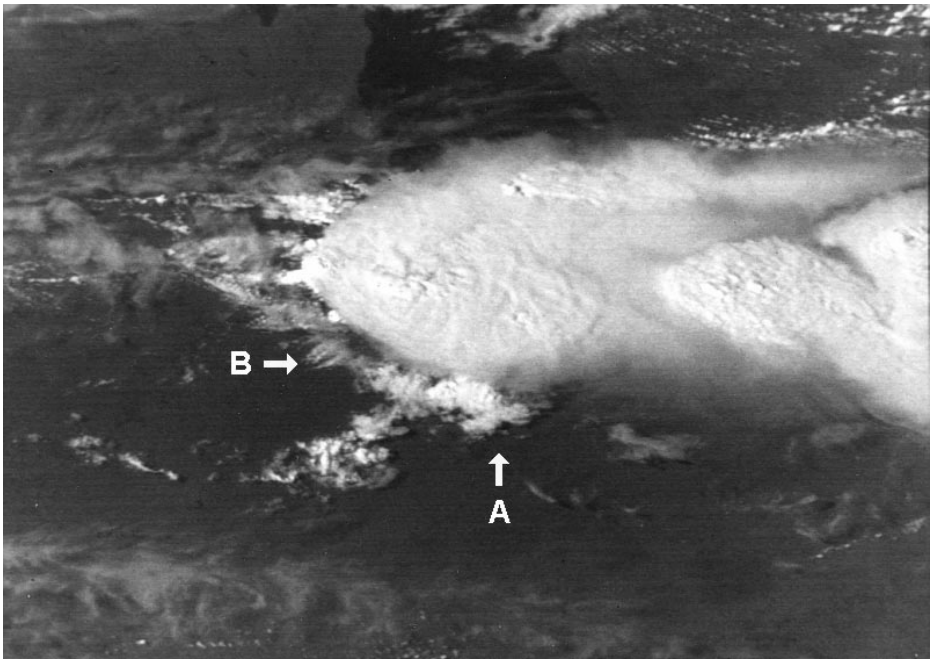

FIG. 3. *GOES-7* visible wavelength view of the inflow region of a tornadic storm near Plainfield, IL, taken at 2101 UTC on 28 Aug 1990. Arrow A points to compact lines of towering cumulus—or feeder clouds—associated with the storm's intense inflow; arrow B points to lines of towering cumulus forming above a newly formed rear-flank downdraft upstream from the primary flanking line.

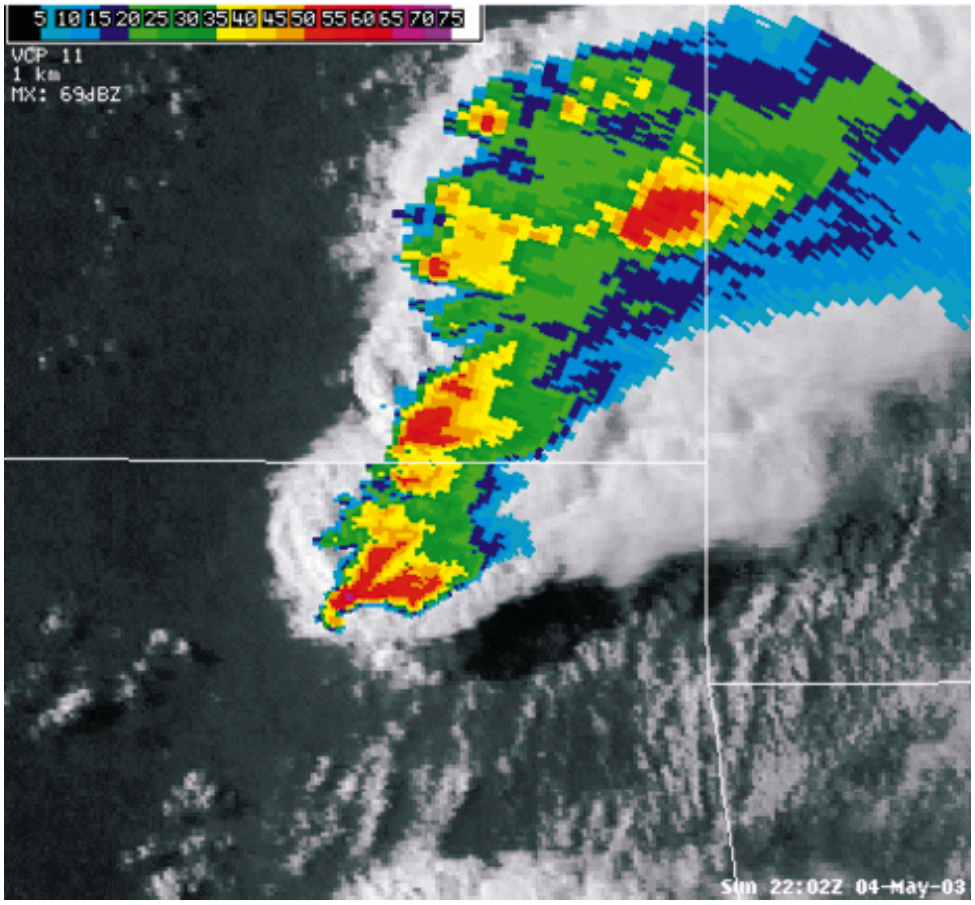

FIG. 4. Visible satellite image from 2202 UTC on 4 May 2003 over northeastern Oklahoma with Tulsa, OK, WSR-88D base reflectivity overlaid. Storm has formed on a dryline and is moving into a region of cloud streets. Velocity data (not shown) confirm that a well-defined mesocyclone is associated with the southernmost storm in this line. Note inflow feeder clouds along the southeastern edge of this core. In this case, no obvious RFD lines are visible.

agery. This note presents a few examples of certain features that seem to be a reflection of severe thunderstorm behavior. Specifically, the appearance of these cloud features seems to coincide with the transition to, or intensification of, supercell thunderstorms. The purpose of presenting these examples is twofold. First, the authors intend to increase awareness among severe storm meteorologists of these important storm characteristics. Second, we would like to generate community interest in discovering the mechanisms by which they are formed.

2. Flanking lines, rear-flank downdrafts, and inflow feeder bands

Three components of severe thunderstorms that can frequently be seen on visible satellite imagery are described in this section. These include the flanking line, organized lines of cumulus congestus above the rear-flank downdraft, and inflow feeder bands.

The flanking line has been a recognized part of severe-thunderstorm nomenclature for many years (Lemon 1976; Doswell 1985; Bluestein 1986; Moller et al. 1994). The flanking line appears as a band of rapidly growing cumulus congestus that merges into the updraft region of the severe storm. It is often located, both in nature and in numerical simulations, above a storm-relative, quasi-stationary outflow boundary at the surface (Lemon 1976; Rotunno and Klemp 1985). This feature is illustrated schematically in Fig. 1 as it relates both to an idealized, low-level radar reflectivity core and to the associated visible cloud.

Organized lines of towering cumulus have also been observed above the rear-flank downdraft (RFD) of severe thunderstorms (Fig. 1). They form above the rain-cooled outflow and are separate from the flanking line. These lines were shown without comment in Purdom and Scofield (1986) (see their Fig. 7.12) and presented with discussion in Weaver and Purdom (1995) and Weaver et al. (2002). Figure 3 from Weaver and Purdom (1995) is reproduced herein as Fig. 2. The arrow labeled ''B'' points to cumulus lines that had just formed above

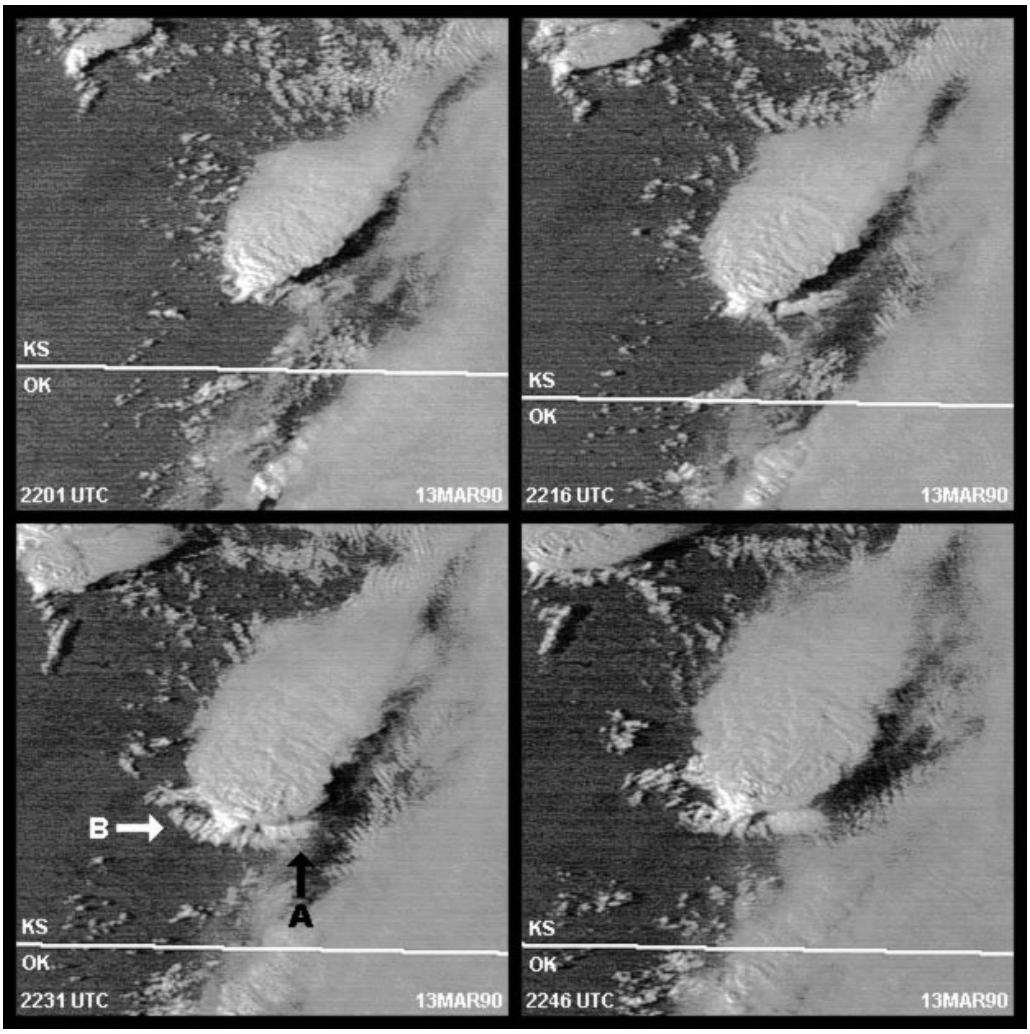

FIG. 5. *GOES-7* visible satellite imagery from 13 Mar 1990 showing the evolution of the thunderstorm from Fig. 2. (upper left) The storm just before the RFD develops (2201 UTC); (upper right) inflow feeder clouds beginning to develop (2216 UTC); (lower left) as in Fig. 2; and (lower right) storm structure at the time an F5 tornado has been on the ground for 12 min (2246 UTC).

an invigorated rear-flank downdraft. Little is known concerning the specific mechanism by which these lines form, but our observations suggest that they seem to appear soon after the RFD forms or intensifies.

Short, compact lines of towering cumulus have also been observed in the region of the inflow of supercell thunderstorms (Fig. 3 of Weaver et al. 1994 and Fig. 2 herein). These inflow feeder clouds appear frequently on visible imagery (e.g., Figs. 3 and 4) but have received little attention in the literature. As with the RFD towering cumulus lines, little is know concerning the mechanisms by which these inflow clouds form. Figure 4 shows 0.5°, base reflectivity from the Tulsa, Oklahoma, Weather Surveillance Radar-1988 Doppler (WSR-88D) for 2202 UTC on 4 May 2003 overlaid on a visible satellite image. Velocity data (not shown) confirm that a well-defined mesocyclone was associated with the southernmost storm. No attempt has been made to adjust the visible imagery for anvil top displacement, since we are concerned herein with low-level storm features. In this case, inflow feeder clouds and the flanking line are clearly visible, though no cloud lines are seen over the outflow area on the west (left) side of the storm.

Figure 5 shows a four-panel time progression of visible satellite data from 13 March 1990. It illustrates how these features develop visually. A flanking line is evident at all four times, but enhanced cloudiness in the inflow region on the southeastern side of the storm can be seen at 2216 UTC. Inflow feeder bands and towering cumulus above the invigorated RFD are evident at 2231 UTC. Large hail was first reported at 2218 UTC, almost coincident with the appearance of the enhanced inflow cloudiness, and an F5 tornado touched down at 2234 UTC (NCDC 1990). In this case, the formation of these

cloud features signaled the supercell's rapid intensification and production of severe weather.

3. Topics for future research

Meteorologists, utilizing satellite imagery to study the near-storm environment of severe thunderstorms, have for some time been aware of features outside the precipitation regions of the cumulonimbus that signify transition to, or intensification of, supercell storms. The ability to view these features may be hampered by intervening anvil, and they are generally not visible at night. However, when observed, they are often a harbinger of severe weather. Though the flanking line is well documented, organized lines of convection above the RFD, and those that frequently appear in the vicinity of a supercell's updraft, are not. Appearing as they do near regions of intense vertical motion, a direct link to internal storm circulation is suggested. By showing a few examples of these phenomena, we hope to generate interest in the research community in learning by what mechanisms such features form and how they relate to supercell behavior. Future field research efforts might include 1) pressure measurements southeast of the wall cloud to document possible correlations with inflow cloud development, 2) wind and pressure measurements to the west of the main precipitation core to document relationships between the developing RFD and multiple cloud lines, and 3) cloud photography and/or videography, from the middle distance (e.g., 10–30 km), both east and west, of a supercell storm to record how these features develop in real time, from a ground-based perspective. A climatological study similar to that by McCann (1983) concerning the relationship between the enhanced-V and severe weather might also be considered for these low-level features. Finally, future theoretical research using high-resolution numerical models might focus on replicating these cloud features and diagnosing the mechanisms leading to their formation, intensification, and dissipation.

Acknowledgments. All severe thunderstorm research at CIRA is sponsored by NOAA Grant NA17RJ1228. The authors would like to express their deepest gratitude to Dr. John Knaff and Mr. Jack Dostalek (CIRA) for their helpful comments on this submission.

REFERENCES

Adler, R. F., and R. A. Mack, 1986: Thunderstorm cloud top dynamics as inferred from satellite observations and a cloud top parcel model. *J. Atmos. Sci.,* **43,** 1945–1960.

Bikos, D. E., J. F. Weaver, and B. C. Motta, 2002: A satellite perspective of the 3 May 1999 Great Plains Tornado Outbreak within Oklahoma. *Wea. Forecasting,* **17,** 635–646.

Bluestein, H. B., 1986: Visual aspects of the flanking line in severe thunderstorms. *Mon. Wea. Rev.,* **114,** 788–795.

Browning, P., J. F. Weaver, and B. Connell, 1997: The Moberly, Missouri, tornado of 4 July 1995. *Wea. Forecasting,* **12,** 915–927.

Doswell, C. A., 1985: The operational meteorology of convective weather. Vol. II, Storm scale analysis, NOAA Tech. Memo. ERL ESG-15, 239 pp. [Available from the National Severe Storms Laboratory, 1313 Halley Circle, Norman, OK 73069.]

Heymsfield, G. M., R. H. Blackmer Jr., and S. Schotz, 1983: Upper-level structure of Oklahoma tornadic storms on 2 May 1979. I: Radar and satellite observations. *J. Atmos. Sci.,* **40,** 1740–1755.

Lemon, L. R., 1976: The flanking line, a severe thunderstorm intensification source. *J. Atmos. Sci.,* **33,** 686–694.

McCann, D. W., 1983: The enhanced-V: A satellite observable severe storm signature. *Mon. Wea. Rev.,* **111,** 887–894.

Moller, A. R., C. A. Doswell III, M. P. Foster, and G. R. Woodall, 1994: The operational recognition of supercell thunderstorm environments and storm structures. *Wea. Forecasting,* **9,** 327–347.

NCDC, 1990: *Storm Data.* Vol. 32, No. 3, 114 pp. [Available from National Climatic Data Center, 151 Patton Ave., Asheville, NC 28801-5001.]

Purdom, J. F. W., 1976: Some uses of high-resolution GOES imagery. *Mon. Wea. Rev.,* **104,** 1474–1483.

——, 1983: Subjective interpretation of geostationary satellite data for nowcasting. *Nowcasting,* K. A. Browning, Ed., Academic Press, 149–166.

——, and R. Scofield, 1986: The use of satellite data for mesoscale analyses and forecasting applications. *Mesoscale Meteorology and Forecasting,* P. S. Ray, Ed., Amer. Meteor. Soc., 118–150.

Rotunno, R., and J. Klemp, 1985: On the rotation and propagation of simulated supercell thunderstorms. *J. Atmos. Sci.,* **42,** 271–292.

Setvák, M., and C. A. Doswell III, 1991: The AVHRR channel 3 cloud top reflectivity of convective storms. *Mon. Wea. Rev.,* **119,** 841–847.

Weaver, J. F., 1980: Storm detection: Satellites. *McGraw-Hill Encyclopedia of Ocean and Atmospheric Sciences,* S. P. Parker, Ed., McGraw-Hill, 457–460.

——, and S. P. Nelson, 1982: Multiscale aspects of thunderstorm gust fronts and their effects on subsequent storm development. *Mon. Wea. Rev.,* **110,** 707–718.

——, and J. F. W. Purdom, 1995: An interesting mesoscale storm–environment interaction observed just prior to changes in severe storm behavior. *Wea. Forecasting,* **10,** 449–453.

——, ——, and E. J. Szoke, 1994: Some mesoscale aspects of the 6 June 1990 Limon, Colorado, tornado case. *Wea. Forecasting,* **9,** 45–61.

——, J. F. Dostalek, B. C. Motta, and J. F. W. Purdom, 2000: Severe thunderstorms on 31 May 1996: A satellite training case. *Natl. Wea. Dig.,* **23,** 3–19.

——, J. A. Knaff, D. E. Bikos, G. Wade, and J. M. Daniels, 2002: Satellite observations of a severe supercell thunderstorm on 24 July 2000 made during the *GOES-11* science test. *Wea. Forecasting,* **17,** 124–138.